Environment and Natural Resources Journal

Volume 23
Issue 3
2025

Assessing Spatial-Temporal Patterns of Agricultural Drought Vulnerability and Its Impacts on Economic Crops, Nakhon Ratchasima, Thailand

Suwit Ongsomwang*

School of Mathematics and Geoinformatics, Institute of Science, Suranaree University of Technology, Nakhon Ratchasima 3000, Thailand

ARTICLE INFO

Received: 18 Nov 2024
Received in revised: 14 Mar 2025
Accepted: 17 Mar 2025
Published online: 8 Apr 2025
DOI: 10.32526/ennrj/23/20240304

Keywords:
Agricultural drought exposure/ Agricultural drought sensitivity/ Adaptive capacity/ Agricultural drought vulnerability/ Potential drought impact

*** Corresponding author:**
E-mail: suwit@sut.ac.th

ABSTRACT

Thailand frequently suffers from rainfall shortages and ensuing droughts and the northeast region is especially vulnerable. The effects of climate change on water resources are further directly related to agricultural drought vulnerability. The objectives of the study were (1) to assess the spatial and temporal patterns of agricultural drought vulnerability based on agricultural drought exposure, agricultural drought sensitivity, and adaptive capacity and (2) to assess the potential impact of agricultural drought vulnerability on economic crops. To do so, this study integrated drought exposure, drought sensitivity and adaptive capacity for assessing spatial and temporal patterns of agricultural drought vulnerability and their potential impacts on economic crops at both the district and subdistrict levels in Thailand's northeastern Nakhon Ratchasima Province. Our results showed that the spatial and temporal patterns of agricultural drought vulnerability in two periods (6m10 and 12m) varied from one region to another. Levels of severity were established, and moderate, high and very high levels were found in 10 districts and 96 subdistricts in the 6m10 period (May to October). They further occurred in 17 districts and 166 subdistricts in the 12m period (January to December). Districts and subdistricts with identical potential impact in both periods included 3 districts and 48 subdistricts. The potential impact of agricultural drought vulnerability on economic crops further was higher in the 12m duration than for 6m10. The highest potential impact was found to be on cassava (2023). In conclusion, the results of the study can be used as basic information for government agencies to monitor and mitigate agricultural drought in Nakhon Ratchasima. The government should further consider implementing a feasibility study for groundwater use in local agriculture, to better mitigate the impact of drought on important vulnerable economic crops.

1. INTRODUCTION

Drought is a complex phenomenon because of its unpredictable start and end, the length of the event, as well as its nonspecific spatial extent (or geographic reach) and both uncertain frequency and intensity. Gordon (1992) stated that drought lacks straightforward entry, duration, and termination points, making it challenging to analyze. According to the United Nations Convention to Combat Desertification (UNCCD) drought has multiple negative impacts, even within a single domain (2023). Drought most severely impacts ecosystems with homogeneous vegetation, which are most susceptible, and especially so under long-term conditions (Ding et al., 2020). The impacts of drought are intensified by their diverse effects across different sectors, including rivers, watercourses, agriculture, electricity production, and industry - leading to significant implications for gross domestic product and international welfare (Begum et al., 2022).

Citation: Ongsomwang S. Assessing spatial-temporal patterns of agricultural drought vulnerability and its impacts on economic crops, Nakhon Ratchasima, Thailand. Environ. Nat. Resour. J. 2025;23(3):265-278. (https://doi.org/10.32526/ennrj/23/20240304)

Thailand frequently suffers from droughts due to rainfall shortages, as well as reduced flow in surface and sub-surface rivers, and poor land management practices. The entire country was affected by severe droughts in 1979, 1994, and 1999 - and the northeastern region, which has the highest poverty rates, remains particularly vulnerable (World Bank Group, 2023).

Conceptually, vulnerability is a relative measure, and it indicates the degree to which a system is susceptible to damage (harm) due to the occurrence of an event (Smit et al., 1999). Most of the definitions of vulnerability originate from two approaches: climate change adaptation (CCA) and disaster reduction risk (DRR) (González Tánago et al., 2016). Many researchers have conducted vulnerability assessments related to the effect of climate change according to the CCA approach (Chandrasekar et al., 2009; Fontaine and Steinemann, 2009; Antwi-Agyei et al., 2012; De Stefano et al., 2015; Murthy et al., 2015; Dabanli, 2018; Hoque et al., 2021; Gao et al., 2023; Mulyanti et al., 2023; Babel et al., 2024; Senapati and Das, 2024).

Therefore, the framework of Fontaine and Steinemann (2009), including drought exposure, drought sensitivity, and adaptive capacity, was here applied to assess agricultural drought vulnerability using geospatial analysis. The specific objectives of the study were (1) to assess the spatial and temporal patterns of agricultural drought vulnerability based on agricultural drought exposure, agricultural drought sensitivity, and adaptive capacity and (2) to assess the potential impact of agricultural drought vulnerability on economic crops.

2. METHODOLOGY

2.1 Study area

The study area is Nakhon Ratchasima Province, which covers 20,729 km^2 (Figure 1). There are 12 Sub-Basins in the study area.

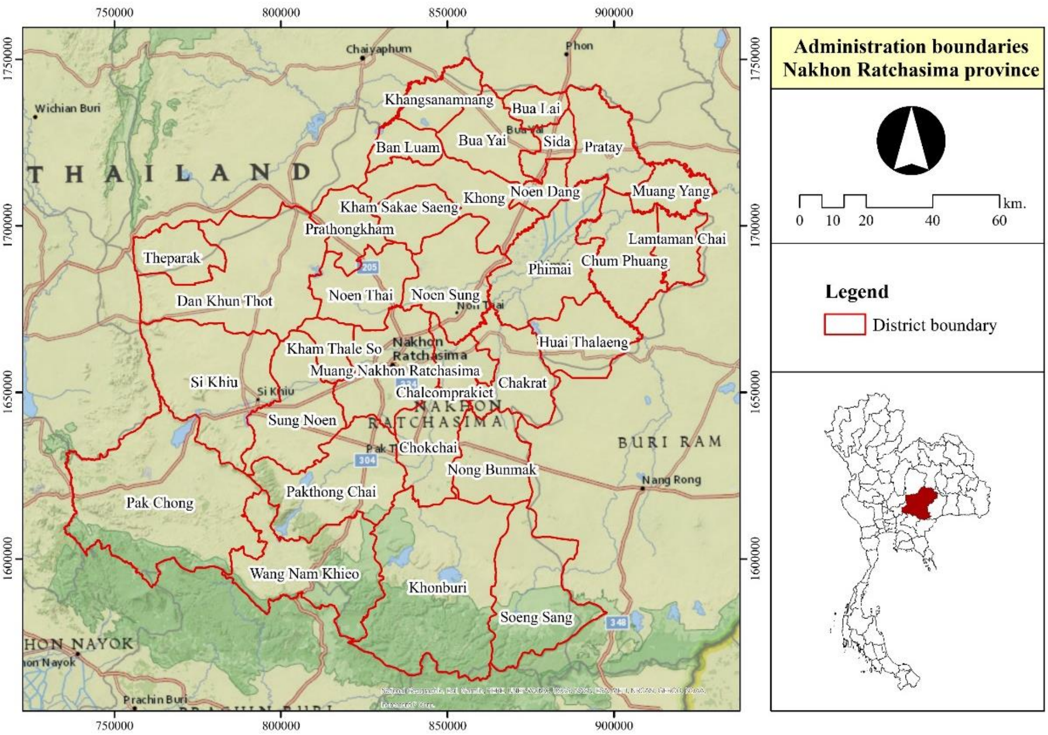

Figure 1. Location map of the study area

2.2 Data

Data collected and prepared for assessing agricultural drought vulnerability included agricultural drought exposure, agricultural drought sensitivity and adaptive capacity components, all summarized below.

- Rainfall data from 1975 to 2022 from 37 stations for SPI calculation
- MOD31A-NDVI product from 2002 to 2022 for VCI extraction
- MOD11B-LST product from 2002 to 2022 for LST extraction

- SRTM DEM for landform and elevation extraction
- Land use data in 2008, 2011, 2015, 2017, 2019, and 2023 for land use extraction
- Soil series for soil drainage extraction
- Agricultural irrigation area
- Waterbody data from 2023 for Euclidean distance calculation
- River network and sub-basin boundary for drainage density calculation
- Average rice harvested area from 2011 to 2023
- Number of rice farmer households in 2023
- Population data in 2023
- Potential groundwater yield

Figure 2 displays the workflow of the research methodology. Brief information is summarized below.

2.3 Assessing agricultural drought exposure (ADE)

ADE was assessed by combining the meteorological drought frequency (MDF) and meteorological drought intensity (MDI) indices of the 2 given periods (6m10 and 12m) using a multiplication operation. For the MDF index, monthly rainfall data (1975-2022) from 37 stations were used to calculate the standardized precipitation index (SPI) in the 2 periods. This was done using Equation 1, with four drought levels: near normal drought (NND), moderate drought (MD), severe drought (SD) and extreme drought (ED), as suggested by McKee et al. (1993) (Table 1).

$$SPI_i = (X_i - X_{mean})/\sigma \tag{1}$$

Where; X_i is standardized rainfall of a given station for period i; X_{mean} and σ are the long-term mean and standard deviation of standardized rainfall for the same period.

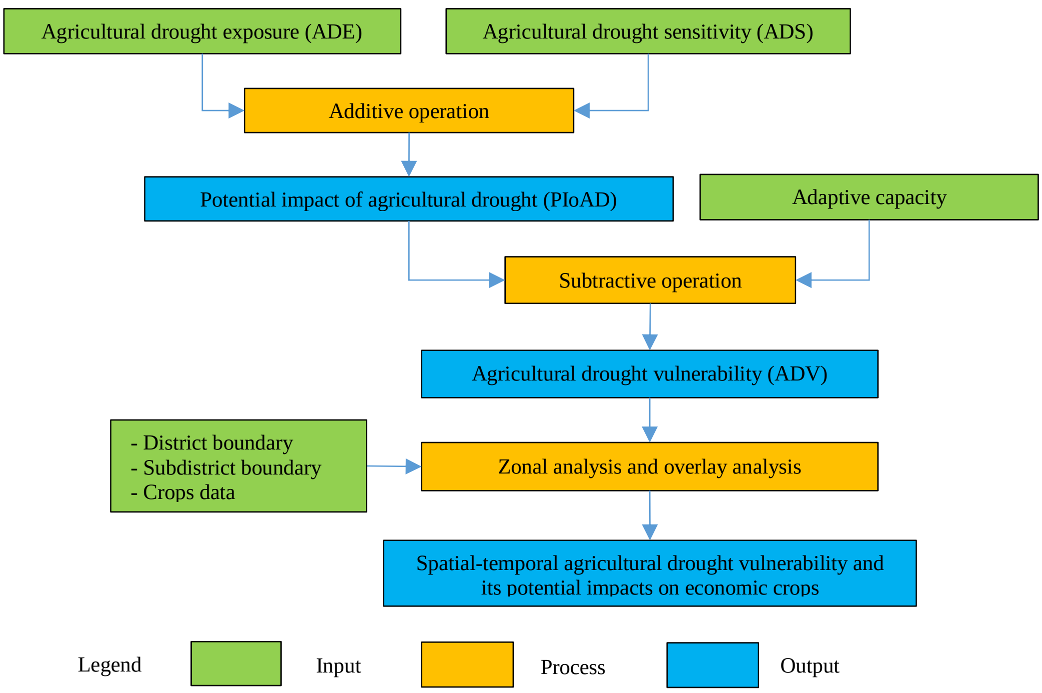

Figure 2. Research methodology workflow

Table 1. Drought classification based on SPI

Level of drought	SPI value	Weights
Near-normal drought (NND)	0 to -0.99	1
Moderate drought (MD)	-1.00 to -1.49	2
Severe drought (SD)	-1.50 to -1.99	3
Extreme drought (ED)	-2.00 and less	4

Thereafter, the probability of drought occurrence (DOc) at each station for each SPI period (6m10 and 12m) and drought level (NND, MD, SD, and ED) was calculated by taking the ratio between counting number in each drought level to the total number of years (48 years) (Sönmez et al., 2005). The

DOc values of 73 stations for each SPI period in each drought level were separately interpolated to create continuous surface data using the Inverse Distance Weighted (IDW) method, as suggested by Tadesse et al. (2010). Later, the interpolated probability of DOc for each period and for each drought level was reclassified into four levels: low, moderate, high, and very high, using the natural break (NB) method, and by assigning ratings for each level (with a value of 1, 2, 3, and 4, respectively). The MDF index of each period, with an accompanying drought severity category, was integrated using Simple Additive Weighting (SAW) (Kaliszewski and Podkopaev, 2016) as:

$$\mathrm{MDFI_{Met}} = (\mathrm{NND_r} \times \mathrm{NND_w}) + (\mathrm{MD_r} \times \mathrm{MD_w}) + (\mathrm{SD_r} \times \mathrm{SD_w}) + (\mathrm{ED_r} \times \mathrm{ED_w}) \quad (2)$$

Where; $MDFI_{Met}$ is the meteorological drought frequency index of a specific time, NND_r is the rating of NND occurrence, NND_w is the weight of NND occurrence, MD_r is the rating of MD occurrence, MD_w is the weight of MD occurrence, SD_r is the rating of SD occurrence, SD_w is the weight of SD occurrence, ED_r is the rating of ED occurrence, ED_w is the weight of ED occurrence.

Meanwhile, the MDI index is considered to be the degree of the precipitation deficiency and the severity of drought measurement (as determined by SPI, when it is less than -1 and equals -1 for the specific period). The MDI index of each period at each station was extracted based on SPI values less than or equal to -1 (Sehgal and Dhakar, 2016) and the extracted MDI values for each period at the 37 stations were separately interpolated to create the MDI index using the IDW method.

Finally, the MDF and MDI indices were combined by multiplication for the MDE index and reclassified into five MDE severity levels (very low, low, moderate, high, and very high) using the NB method. (See the workflow of MDE in Figure 3). Spatial distribution of the MDF, MDI and MDE indices for MDE classification in 2 periods (6m10 and 12m) are displayed in Figure 4.

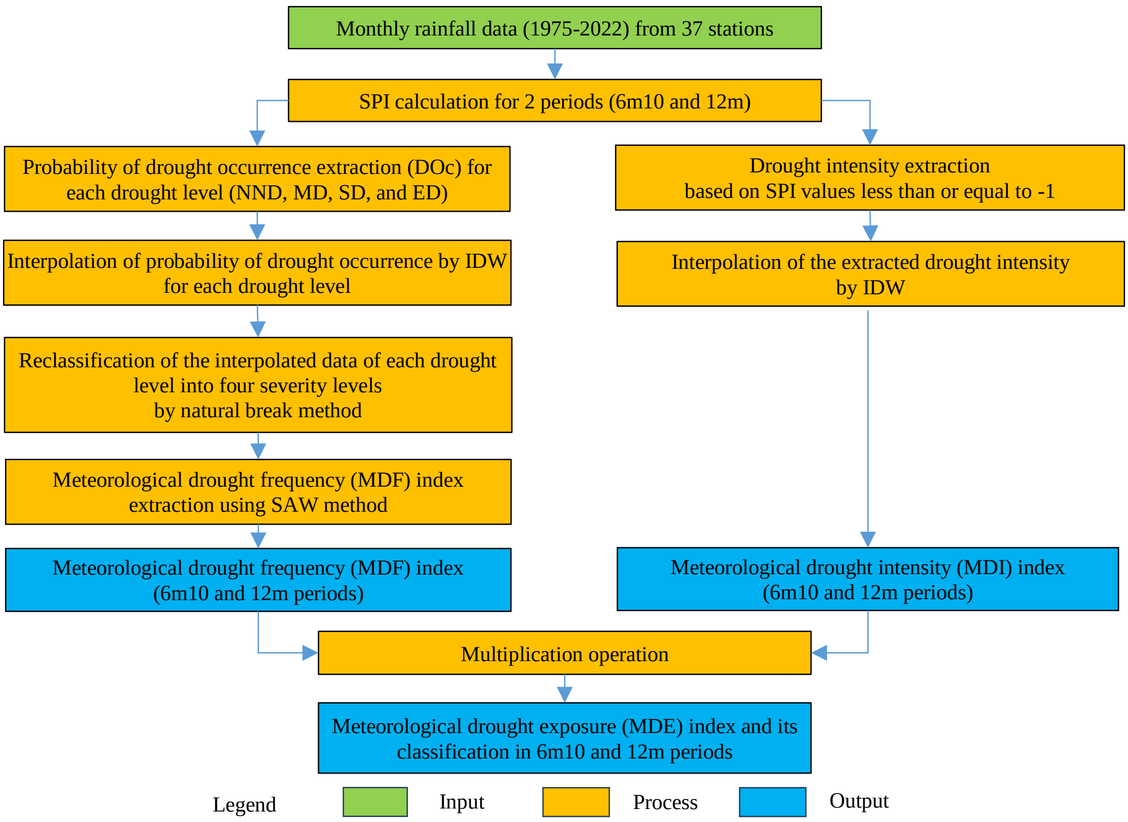

Figure 3. Workflow of agricultural drought exposure assessment

2.4 Assessing agricultural drought sensitivity (ADS)

ADS was assessed using a weighted linear combination (WLC) method with the analytical hierarchical process (AHP) based on selected factors under four conditions: vegetation, climate, physical and socio-economic (Figure 5).

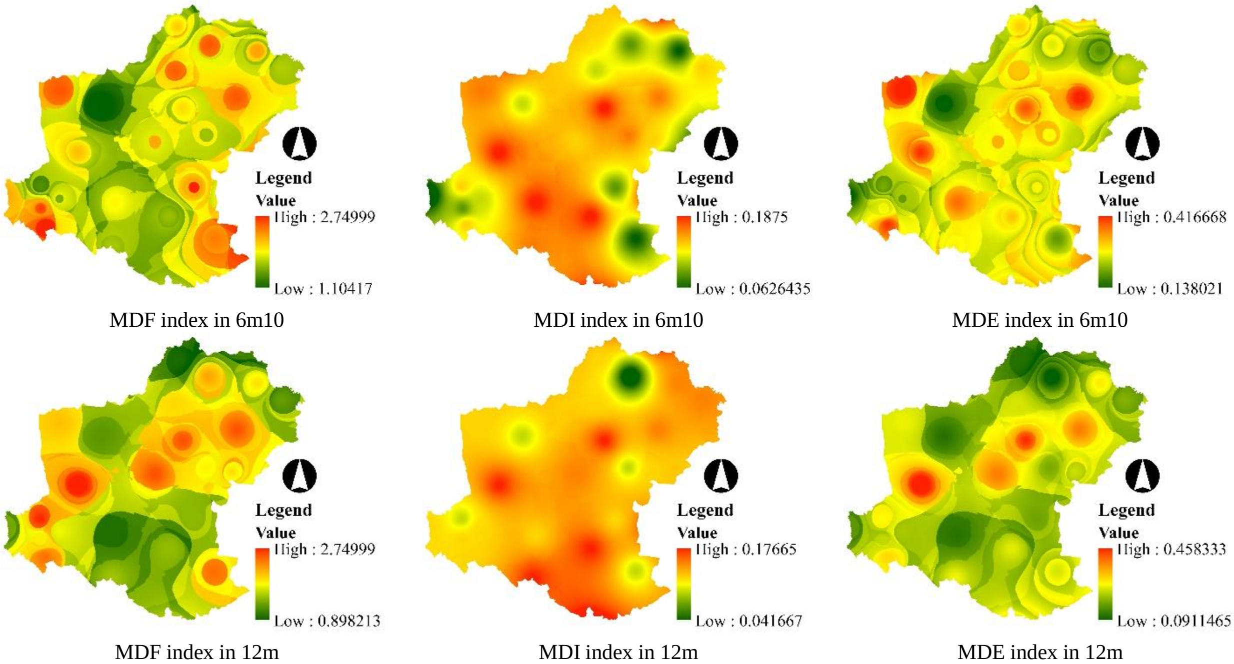

Figure 4. Spatial distribution of the MDF, MDI and MDE indices for MDE classification in 2 periods.

(1) Vegetation condition: Two factors representing vegetation conditions for ADS are agricultural drought frequency (ADF) and agricultural drought intensity (ADI). This study identified ADF based on the vegetation condition index (VCI) computed using the normalized difference vegetation index (NDVI) from MOD31A-NDVI products over a phenology period (May-October) from 2002 to 2022 using Equation 3. If VCI values are 100%, it indicates healthy vegetation conditions. In contrast, VCI values near 0%, identify poor vegetation conditions (Kogan, 1995).

$$VCI=100*\frac{(NDVI_i\text{-}NDVI_{min})}{(NDVI_{max}\text{-}NDVI_{min})} \qquad (3)$$

Where; $NDVI_i$ is the filtered NDVI image in the phenology period, $NDVI_{max}$ is the multi-year maximum NDVI in the phenology period, and $NDVI_{min}$ is the multi-year minimum NDVI in the phenology period.

Since it represents vegetation conditions, any VCI equal to or less than 35% in the phenology period was identified as agricultural drought. All VCI images were reclassified with a threshold value of =<0.35 as 1, while other values were reclassified as 0. Thereafter, all reclassified images (1 and 0) were added together and divided by the total number of images (210 images from 21 years) for ADF. The extracted value was reclassified into five rating scores via the NB method.

Meanwhile, ADI was calculated based on average historical VCI values (0-100%) in the phenology period. Herein, all VCI images were reclassified with a threshold value of =< 0.35, while other values were reclassified as 0. Thereafter, all reclassified images were added and averaged by the number of years for ADI. The extracted value was then reclassified into five rating scores by using the NB method.

(2) Climate condition: Two factors that characterize climate conditions for ADS, as suggested by Hayes et al. (2011) and the World Meteorological Organization (WMO) (2012), are average SPI and SPEI (Standardized Precipitation Evapotranspiration Index). Our SPI was calculated and averaged from rainfall data (2002-2022) drawn from 37 stations in the 2 periods. They were interpolated using the IDW method and reclassified into five rating scores by the NB method.

Meanwhile, SPEI, specifically including characteristics of the region's climate (Vicente-Serrano et al., 2010), was calculated based on monthly rainfall and temperature (2002-2022). Herein, monthly rainfall data were retrieved from 37 stations, while average monthly average temperatures were retrieved from MODIS LST data. Monthly rainfall and temperature data were used to calculate the average SPEI of the 2 given periods using the SPEI calculator. They were interpolated using the IDW method and then reclassified into five rating scores via the NB method.

(3) Physical condition: Seven factors characterize physical conditions for ADS. These include land use, agricultural irrigation areas, distance to waterbodies, drainage density, landform, and elevation.

(3.1) Land use: Land use data in 2008, 2011, 2015, 2017, 2019, and 2023 from the Land Development Department (LDD) were reclassified into five rating scores according to land use type, and then averaged to produce five rating scores.

(3.2) Agricultural irrigation area: ADS, according to agricultural irrigation area, was assigned rating scores for irrigated and rain-fed agricultural areas.

(3.3) Distance to water bodies: Areas closer to waterbodies are less vulnerable to water shortages because of more recharge potential (Jain et al., 2015). Euclidean distance was utilized to calculate the distance to water bodies, and these values were then reclassified into five rating scores by the NB method.

(3.4) Drainage density: Drainage density values were calculated using the total length of stream channels in a drainage basin divided by the surface area of the basin (Pandey et al., 2010). These were then classified into five rating scores by using the NB method.

(3.5) Soil drainage: Soil drainage properties were sorted by soil series obtained from the LDD and then reclassified into five rating scores, as Prathumchai et al. (2001) suggested.

(3.6) Landform: Landform classification was based on the percentage of slope (Land Development Department, 2009) and then reclassified into five rating scores.

(3.7) Elevation: The elevation classification was extracted using DEM, according to LDD standards (2009) and then reclassified into five rating scores.

(4) Socio-economic condition: Socio-economic factors include average areas of harvested rice (2011-2023), farmer households in 2023 and population density in 2023 at the subdistrict level.

(4.1) Average rice harvested area: Average rice harvested areas (2011-2023) were determined at the subdistrict level, then calculated and reclassified into five rating scores by using the NB method.

(4.2) Number of farmer households: The number of farmer households is sensitive to agricultural drought (Pei et al., 2016). Areas are also more vulnerable when the proportion of farmer households increases. The number of farmer households in 2023 was extracted and reclassified into five rating scores by using the NB method.

(4.3) Population density: Shahid and Behrawan (2008) applied population density measurements to assign agricultural drought sensitivity scores. Population densities in 2023 were extracted and reclassified into five rating scores via the NB method.

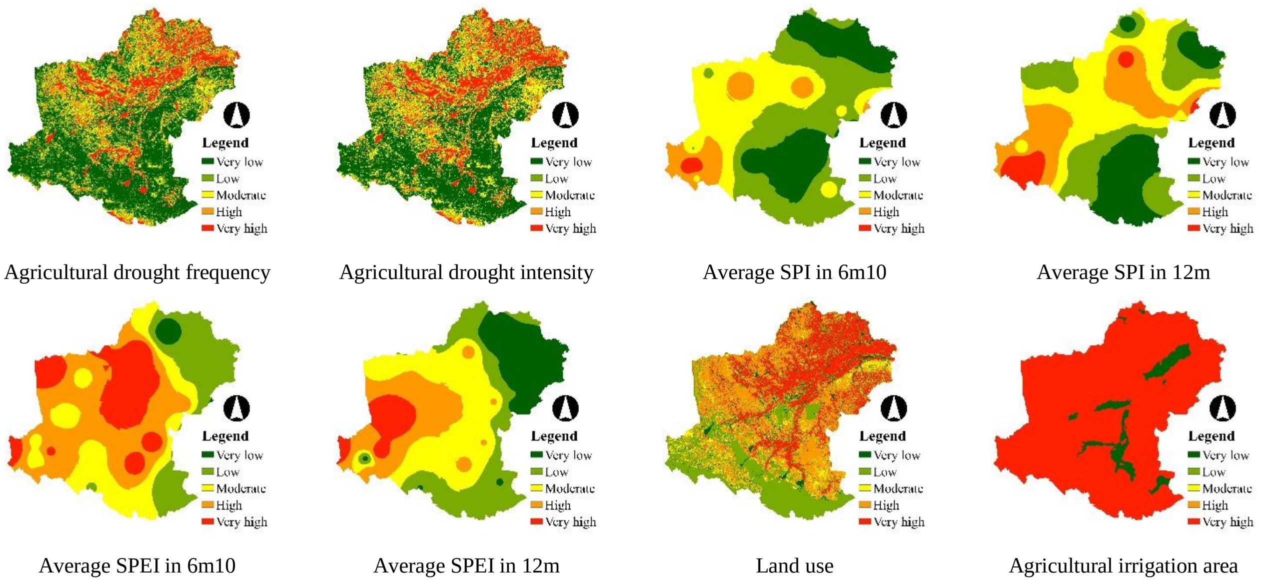

Figure 5. Spatial distribution of ADS assessment factors

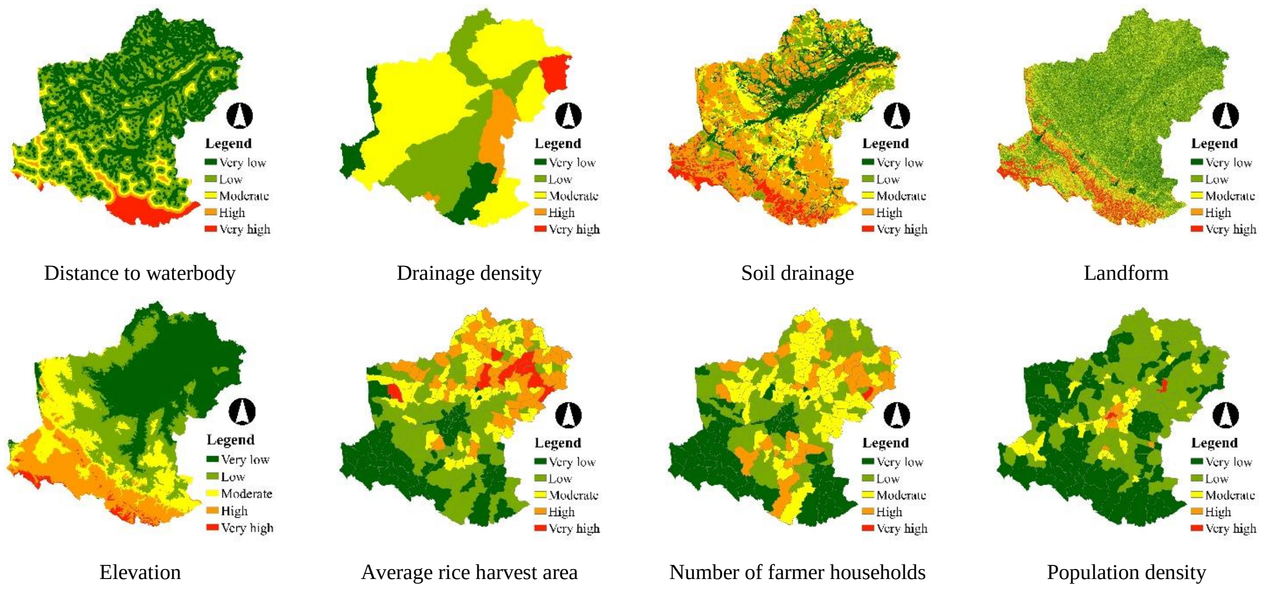

Figure 5. Spatial distribution of ADS assessment factors (cont.)

Since all ADS factors have different units, the rating score for each factor was normalized into a shared standard using a standardized ranking value (Tsangaratos et al., 2013):

$$v = a + (b - a)* \left[\frac{V - A}{B - A}\right] \quad (4)$$

Where; v is the new rating value that is between a and b, V is the original rating value that is between A and B, A is the minimum for original rating values, B is the maximum for original rating values, a is the new minimum of standardized rating values, and b is the new maximum of standardized rating values.

In this study, the minimum original rating value (A) is 1, and the maximum (B) is 5. Meanwhile, the new desired minimum of standardized rating values (a) is 1, and the new desired maximum of standardized rating values is 3.

Thereafter, the weight of each factor on ADS was determined using the AHP based on pairwise comparisons with the standard scale from 1 to 9 (Saaty, 1987). Value 9 indicates that one indicator is extremely important, even more so than the others, while value 1 indicates equal importance. The AHP was implemented by generating a pairwise comparison matrix and calculating its principal eigenvector directly to produce the best-fit set of weights with Weight and MCE modules (Eastman et al., 1995) under IDRISI software.

The normalized rating score and weight of each factor (Table 2) were applied to calculate the ADS index for the 2 given periods using the WLC method (Malczewski, 2000):

$$A_i = \sum_{j=1}^{n} w_j \times a_{ij} \quad (5)$$

Where; A_i is total importance of an alternative when all the criteria are considered simultaneously, and w_j denotes the relative weight of importance of the criterion C_j, and a_{ij} is the performance value of alternative A_i when it is evaluated in terms of criterion C_j.

Finally, the ADS index was reclassified into five severity levels (very low, low, moderate, high, and very high) using the NB method. See the workflow of ADS in Figure 6.

Table 2. Normalized rating and weight for ADS assessment

No	Factor	Normalized rating score					Weight
		Very low	Low	Moderate	High	Very high	
1	Agricultural drought frequency	1	1.5	2	2.5	3	0.1749
2	Agricultural drought intensity	1	1.5	2	2.5	3	0.1749
3	Average SPEI: 6m10 and 12m	1	1.5	2	2.5	3	0.1555
4	Average SPI: 6m10 and 12m	1	1.5	2	2.5	3	0.1510

Table 2. Normalized rating and weight for ADS assessment (cont.)

No	Factor	Normalized rating score					Weight
		Very low	Low	Moderate	High	Very high	
5	Land use	1	1.5	2	2.5	3	0.0820
6	Agricultural irrigation area	1	Not applicable	Not applicable	Not applicable	3	0.0570
7	Distance to waterbody	1	1.5	2	2.5	3	0.0530
8	Drainage density	1	1.5	2	2.5	3	0.0385
9	Soil drainage	1	1.5	2	2.5	3	0.0385
10	Landform	1	1.5	2	2.5	3	0.0239
11	Elevation	1	1.5	2	2.5	3	0.0194
12	Average rice yield	1	1.5	2	2.5	3	0.0115
13	Farmer households	1	1.5	2	2.5	3	0.0110
14	Population density	1	1.5	2	2.5	3	0.0089

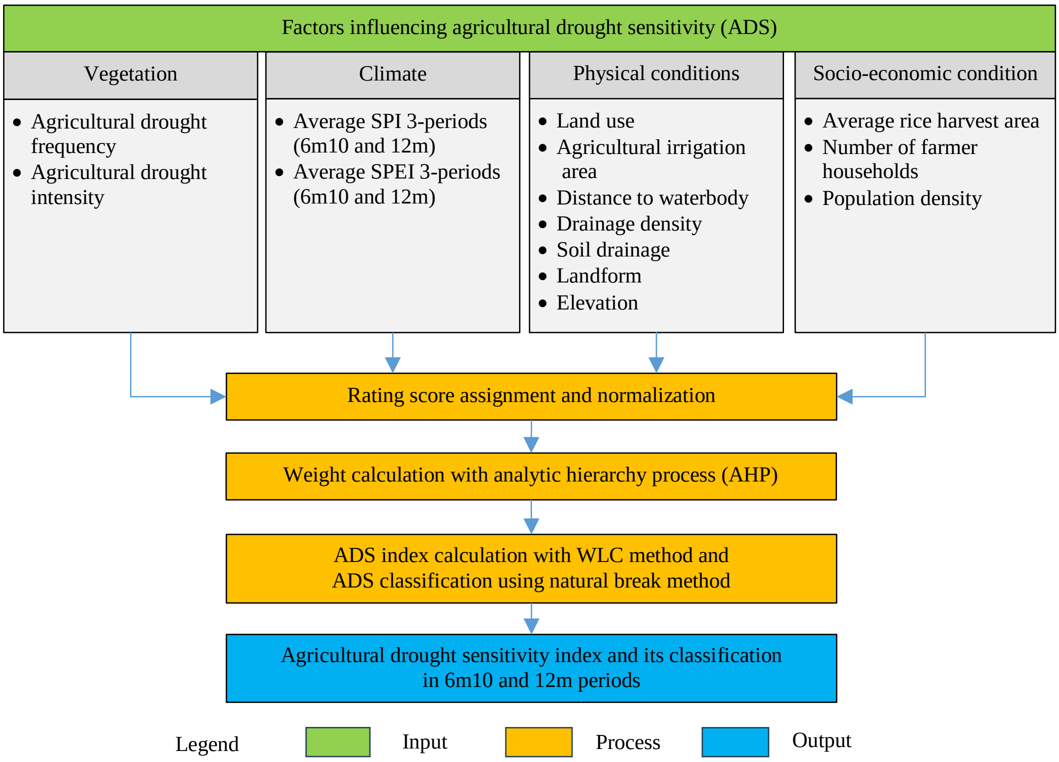

Figure 6. Workflow of agricultural drought sensitivity assessment

2.5 Assessing adaptive capacity

The AC index was assessed using the WLC method (Malczewski, 2000) based on suitability factors for groundwater use in agriculture, including potential groundwater yield, land use in 2023 and landform (Table 3). Finally, the AC index was reclassified into five suitable levels (very low, low, moderate, high, and very high) using the NB method.

2.6 Assessing agricultural drought vulnerability (ADV)

The ADE and ADS were first combined for the Potential Impacts of Agricultural Drought (PIoAD) using additive operation. Then, the derived data was combined with the AC using a subtractive operation for the ADV, and finally reclassified into five severity levels (very low, low, moderate, high, and very high) using the NB method.

Table 3. Rating and weight of suitability factors for groundwater use in agriculture

Suitability	Groundwater yield	Land use types	Landform	Rate
Not suitable	Waterbody	Others land uses	Waterbody	0
Low suitability	Yield < 2 cubic m/hr.	Cassava	Denudational hills and dissected erosion surface	1
Moderate suitability	Yield 2-10 cubic m/hr.	Sugarcane	High terrace	2
Highly suitable	Yield 10-20 cubic m/hr.	Corn	Low and middle terrace	3
Very highly suitable	Yield > 20 cubic m/hr.	Paddy field	Flood plain	4
Weight	3	2	1	

Note: The Waterbody category includes groundwater yield and landform, as surface waters are not considered suitable for groundwater use in agriculture.

2.7 Assessing spatial and temporal patterns of agricultural drought vulnerability and its potential impact on economic crops

The spatial and temporal patterns of ADV at district and subdistrict levels were analyzed according to severity levels using zonal analysis with majority operation. Meanwhile, overlay analysis was applied to identify the potential impacts of ADV on economic crops from LDD's 2023 land use data. Additionally, spatial correlation analysis was applied to characterize the similarity of the patterns.

3. RESULTS AND DISCUSSION

3.1 Potential impacts of agricultural drought (PIoAD)

The spatial and temporal patterns of the PIoAD for the 2 periods were extracted by combining their ADE and ADS (Figures 7(a) to 7(d)). The results are displayed in Figures 7(e) and 7(f). The spatial distribution of high and very high PIoAD in 6m10 occurred in the northwestern portion of the province. Meanwhile, the spatial distribution of high and very high PIoAD in 12m occurred in the northwestern and eastern regions. The spatial patterns of the PIoAD in the 2 periods differed from one region to the next. However, a spatial correlation analysis between the 2 periods showed a strong positive linear relationship, with a value of 0.7172.

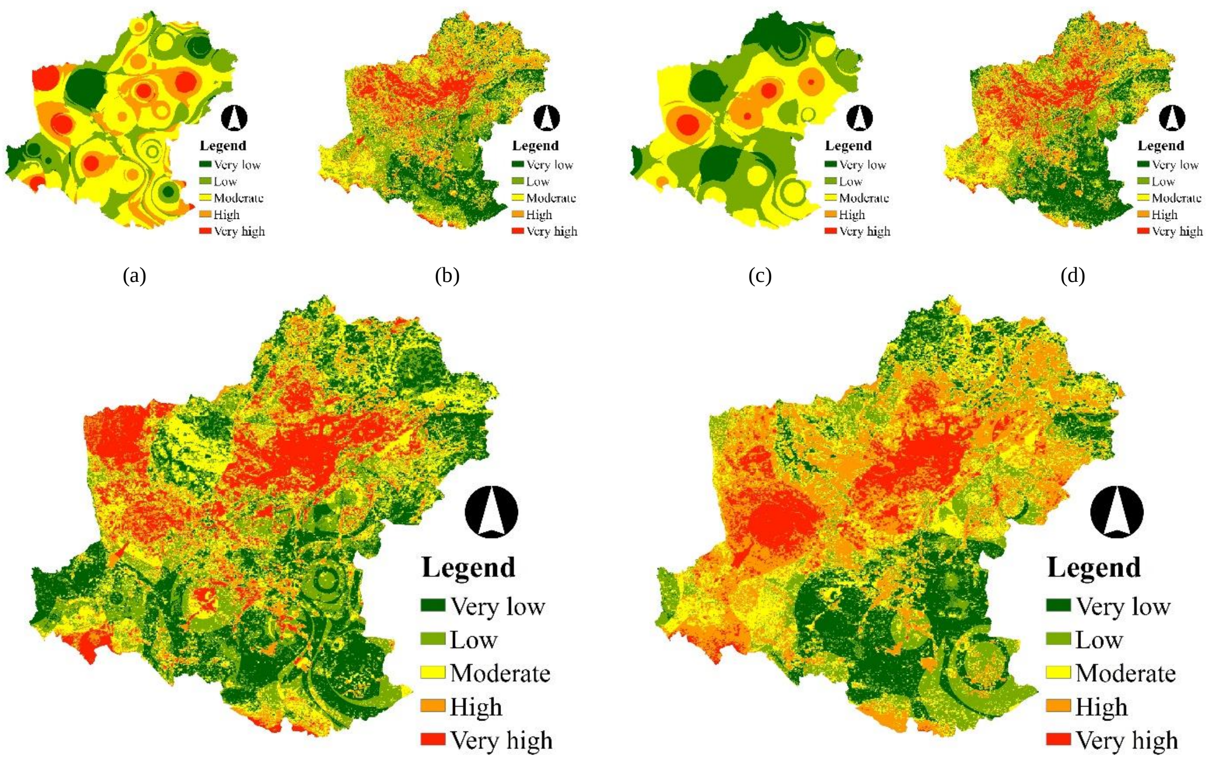

Figure 7. Spatial distribution maps showing (a) ADE in 6m10, (b) ADS in 6m10, (c) ADE in 12m, (d) ADS in 12m, (e) PIoAD classification in 6m10, (f) and PIoAD classification in 12m.

Furthermore, Table 4 reports the number of districts and subdistricts with a majority of severe PIoAD levels in the 2 given periods. In 6m10, combined moderate, high and very high PIoAD severity levels occurred in 18 districts and 146 subdistricts. Meanwhile for 12m, moderate, high and very high levels were found in 21 districts and 204 subdistricts. These results indicated changes in spatial and temporal patterns of PIoAD in both periods. The PIoAD at district and subdistrict levels in 12m were higher than 6m10.

Table 4. Number of districts and subdistricts levels with a majority of severe PIoAD levels in 2 periods

Severity levels of PIoAD	Number of districts and subdistricts			
	6m10 (May-October)		12m (January-December)	
	District	Subdistrict	District	Subdistrict
Very low	8	68	9	51
Low	6	74	2	33
Moderate	12	64	5	39
High	1	21	14	127
Very high	5	61	2	38
Total	32	288	32	288

3.2 Spatial and temporal patterns of agricultural drought vulnerability

The spatial and temporal patterns of ADV, which were extracted by subtraction of the PIoAD in 2 periods (Figures 8(a) and 8(b)) by AC (Figure 8(c)), are displayed in Figures 8(d) and 8(e). The spatial distribution of high and very high ADV in the 6m10 period occurred in the western and southern regions. Meanwhile, the spatial distribution of high and very high ADV in the 12m period occurred in the western region. These findings indicated that spatial and temporal patterns of agricultural drought vulnerability differ from one region to another region over both time periods. A possible reason for these findings is the variation in biophysical and climatic conditions. However, the spatial correlation analysis between the 2 periods showed a strong positive linear relationship, with a value of 0.7568.

Table 5 reports the number of districts and subdistricts accompanied by their ADV severity levels in 2 periods. For 6m10, moderate, high and very high levels of severity occurred in 10 districts and 96 subdistricts. Meanwhile over 12m, moderate, high and very high levels occurred in 17 districts and 166 subdistricts. These results indicated changes in spatial and temporal patterns of ADV in both periods. The potential impact of ADV at moderate, high and very high severity levels in 12m was higher than 6m10. Districts and subdistricts with identical potential ADV impact (moderate, high and very high, in both periods) were found in 3 districts and 48 subdistricts. See details in Table S1 and S2 in Supplementary data. These areas should continue to be monitored for mitigation drought.

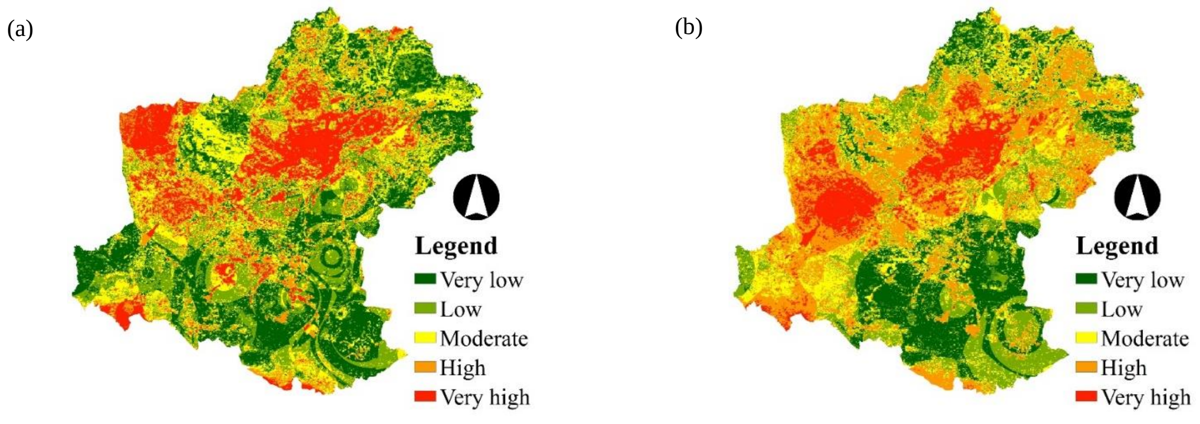

Figure 8. Spatial distribution maps showing (a) potential impact of agricultural drought in 6m10, (b) potential impact of agricultural drought in 12m (c) adaptive capacity (d) agricultural drought vulnerability in 6m10, (e) agricultural drought vulnerability in 12m.

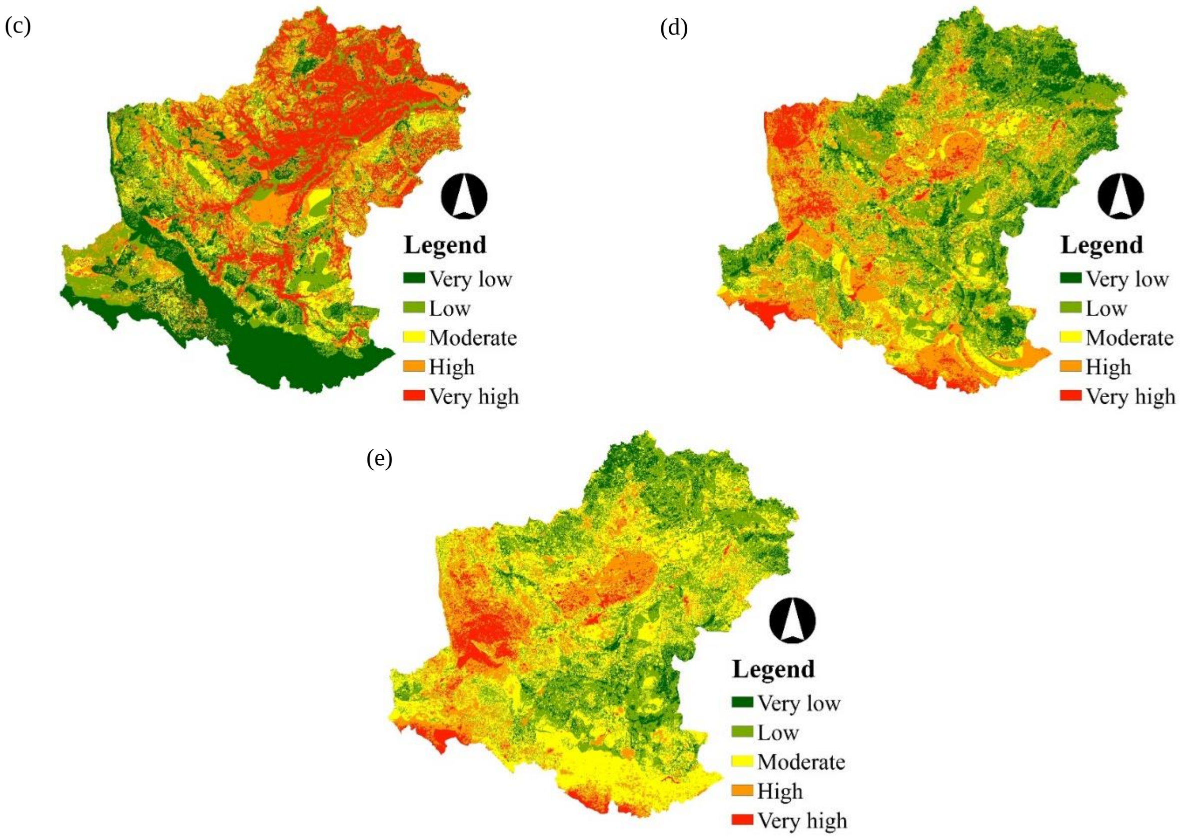

Figure 8. Spatial distribution maps showing (a) potential impact of agricultural drought in 6m10, (b) potential impact of agricultural drought in 12m (c) adaptive capacity (d) agricultural drought vulnerability in 6m10, (e) agricultural drought vulnerability in 12m (cont.).

Table 5. Number of districts and subdistricts with severity levels of ADV in 2 periods

Severity levels of ADV	Number of districts and subdistricts					
	6m10	12m	Duplicate in 2 periods	6m10	12m	Duplicate in 2 periods
	District	District	District	Subdistrict	Subdistrict	Subdistrict
Very low	1	0	0	16	6	1
Low	21	15	13	176	116	98
Moderate	1	15	1	20	120	14
High	8	2	2	68	40	33
Very high	1	0	0	8	5	1
Total	32	32	16	288	288	147

In comparison, the number of districts and subdistricts with moderate, high and very high PIoAD in 6m10 were reduced from 18 to 10 districts and from 146 to 96 subdistricts after applying CA. Likewise, the number of districts and subdistricts with moderate, high and very high PIoAD in 12m was reduced from 21 to 17 districts, and from 204 to 166 subdistricts after applying CA. (See Tables 3 and 4). These findings indicate the significant role of adaptive capacity utilizing groundwater use in agriculture for mitigating agricultural drought. It is recommended that a feasibility study for groundwater use in agriculture be further implemented.

3.3 Potential impacts of agricultural drought vulnerability on economic crops

Table 6 reports the potential impact of ADV in 2 periods on economic crops in 2023. Rice, corn, sugarcane and cassava are all presented according to severity levels. The percentage of the potential impact of ADV with moderate, high, and very high levels in the 6m10 and 12m periods for rice was 28.53% and 41.25% of the total rice area. Meanwhile, the percentage of the potential impact of ADV with moderate, high, and very high levels in 6m10 and 12m periods for corn was 34.97% and 55.74% of the total corn area. The percentage of the potential impact of

ADV with moderate, high, and very high levels in the 6m10 and 12m periods on sugarcane was 32.65% and 41.43% of the total sugarcane area. The percentage of the potential impact of ADV with moderate, high, and very high levels in 6m10 and 12m periods on cassava was 58.92% and 63.77% of the total cassava area. These findings indicate that the potential impact of ADV on economic crops in the 12m period was greater than the 6m10. Besides, the ADV exhibits the highest potential impact on cassava, since the phenological cycle of cassava covers the entire year (2023).

Table 6. Severity level of ADV in 2 periods on economic crops in 2023.

Economic crops	ADV severity level	6m10 (May-October)		12m (January-December)	
		Area (km^2)	Percent	Area (km^2)	Percent
Rice	Very low	1,569.49	25.76	941.94	15.46
	Low	2,785.60	45.72	2,637.54	43.29
	Moderate	973.62	15.98	1,894.23	31.09
	High	756.11	12.41	614.76	10.09
	Very high	7.92	0.13	4.26	0.07
	Total	6,092.73	100.00	6,092.73	100.00
Corn	Very low	182.31	23.28	55.44	7.08
	Low	326.94	41.75	291.16	37.18
	Moderate	122.87	15.69	314.10	40.11
	High	130.23	16.63	118.40	15.12
	Very high	20.75	2.65	3.99	0.51
	Total	783.10	100.00	783.10	100.00
Sugarcane	Very low	394.59	19.26	298.30	14.56
	Low	985.24	48.09	901.65	44.01
	Moderate	348.70	17.02	600.08	29.29
	High	270.64	13.21	220.24	10.75
	Very high	49.58	2.42	28.48	1.39
	Total	2,048.75	100.00	2,048.75	100.00
Cassava	Very low	171.10	4.44	75.53	1.96
	Low	1,411.98	36.64	1,320.26	34.26
	Moderate	902.91	23.43	1,385.77	35.96
	High	979.60	25.42	803.49	20.85
	Very high	388.06	10.07	268.21	6.96
	Total	3,853.65	100.00	3,853.65	100.00

4. CONCLUSION

This study integrated agricultural drought exposure, agricultural drought sensitivity and adaptive capacity for assessing spatial and temporal patterns of agricultural drought vulnerability (ADV) and the potential impact on crops at district and subdistrict levels. The results indicated that the potential impacts of spatial patterns of ADV with moderate, high, and very high severity between January and December (covering 17 districts and 166 subdistricts), were higher than between May and October (with 10 districts and 96 subdistricts). Likewise, the potential impact of agricultural drought vulnerability between January and December on economic crops exhibited more impact than the time between May and October. These results can be used as basic information for government agencies, such as the Department of Agricultural Extension and the Department of Disaster Prevention and Mitigation for monitoring agricultural drought in Nakhon Ratchasima province. The government should further implement a feasibility study for groundwater use in agriculture to mitigate the impact of drought on economic crops.

ACKNOWLEDGEMENTS

The author acknowledges the support of the Fundamental Fund (FF) grant number FF1-103-67-12-06(F) from Thailand Science Research and Innovation, Ministry of Higher Education, Science, Research and Innovation. The author also acknowledges the School of Mathematics and Geoinformatics, Institute of Science, at Suranaree University of Technology, for supporting the facilities to undertake this research.

AUTHOR CONTRIBUTION

Conceptualization, methodology, software, validation, formal analysis, investigation, resources, data curation, writing - original draft preparation and writing-review and editing, visualization, supervision, project administration and funding acquisition, SO.

DECLARATION OF COMPETING INTEREST

The author declares no conflict of interest.

REFERENCES

Antwi-Agyei P, Fraser ED, Dougill AJ, Stringer LC, Simelton E. Mapping the vulnerability of crop production to drought in Ghana using rainfall, yield and socio-economic data. Applied Geography 2012;32(2):324-34.

Begum RA, Lempert R, Ali E, Benjaminsen TA, Bernauer T, Cramer W, et al. Climate Change 2022: Impacts, Adaptation and Vulnerability. Contribution of Working Group II to the Sixth Assessment Report of the Intergovernmental Panel on Climate Change. Cambridge, UK: Cambridge University Press, 2022; p. 121-96.

Babel MS, Chawrua L, Khadka D, Tingsanchali T, Shanmungam MS. Agricultural drought risk and local adaptation measures in the Upper Mun River Basin, Thailand. Agricultural Water Management 2024;292:Article No. 108655.

Chandrasekar K, Sai MS, Roy P, Jayaraman V, Krishnamoorthy R. Identification of agricultural drought vulnerable areas of Tamil Nadu, India using GIS-based multi-criteria analysis. Asian Journal of Environment Disaster Management 2009;1(1):40-61.

Dabanli I. Drought hazard, vulnerability, and risk assessment in Turkey. Arabian Journal of Geosciences 2018;11:Article No. 538.

De Stefano L, Gonza´lez Ta´nago I, Ballesteros M, Urquijo J. Methodological Approach Considering Different Factors Influencing Vulnerability-Pan-European Scale. DROUGHT-R&SPI Technical Report No. 26. 2015. p. 121.

Ding Y, Xu J, Wang X, Peng X, Cai H. Spatial and temporal effects of drought on Chinese vegetation under different coverage levels. Science of the Total Environment 2020;716:Article No. 137166.

Eastman JR, Jin W, Kyem PAK, Toledano J. Raster procedures for multi-criteria/multi-objective decisions. Photogrammetric Engineering and Remote Sensing 1995;61(5):539-47.

Fontaine MM, Steinemann AC. Assessing vulnerability to natural hazards: impact-based method and application to drought in Washington state. Natural Hazards Review 2009;10(1):11-8.

Gao F, Zhang S, Yu R, Zhao Y, Chen Y, Zhang Y. Agricultural drought risk assessment based on a comprehensive model using geospatial techniques in Songnen plain, China. Land 2023;12:Article No. 1184.

González Tánago I, Urquijo J, Blauhut V, Villarroya F, De Stefano L. Learning from experience: A systematic review of assessments of vulnerability to drought. Natural Hazards 2016;80:951-73.

Gordon AH. The random nature of drought: Mathematical and physical causes. International Journal of Climatology 1992;13:497-507.

Hayes M, Svoboda M, Wall N, Widhalm M. The Lincoln declaration on drought indices: Universal meteorological drought index recommended. Bulletin of the American Meteorological Society 2011;92(4):485-8.

Hoque MA, Pradhan B, Ahmed N, Alamri AM. Drought vulnerability assessment using geospatial techniques in Southern Queensland, Australia. Sensors (Basel, Switzerland) 2021;21 Article No. 6896.

Jain VK, Pandey RP, Jain MK. Spatial-temporal assessment of vulnerability to drought. Natural Hazards 2015;76:443-69.

Kaliszewski I, Podkopaev D. Simple additive weighting-A metamodel for multiple criteria decision analysis methods. Expert Systems with Applications 2016;54:155-61.

Kogan FN. Droughts of the late 1980s in the United States as derived from NOAA polar-orbiting satellite data. Bulletin of the American Meteorological Society 1995;76(5):655-68.

Land Development Department (LDD). Land Use Plans, Lamtakhong Watershed. Land Office of Soil Survey and Land Use Planning, Land Development Department; 2009. p. 206 (in Thai).

Malczewski J. On the use of weighted linear combination method in GIS: Common and best practice approaches. Transactions in GIS 2000;4(1):5-22.

McKee TB, Doesken NJ, Kleist J. The relationship of drought frequency and duration to time scales. Proceedings of the 8th Conference on Applied Climatology; 1993 Feb 17-23; Anaheim, CA. Boston, MA, American Meteorological Society; 1993.

Mulyanti H, Istadi I, Gernowo R. Assessing vulnerability of agriculture to drought in East Java, Indonesia: Application of GIS and AHP. Geoplanning: Journal of Geomatics and Planning 2023;10(1):55-72.

Murthy CS, Laxman B, Sesha Sai MVRS. Geospatial analysis of agricultural drought vulnerability using a composite index based on exposure, sensitivity and adaptive capacity. International Journal of Disaster Risk Reduction 2015;12: 163-71.

Pandey S, Pandey AC, Galkate RV, Byun HR, Mal BC. Integrating hydro-meteorological and physiographic factors for assessment of vulnerability to drought. Water Resources Management 2010;24:4199-217.

Pei W, Fu Q, Liu D, Li T, Cheng K. Assessing agricultural drought vulnerability in the Sanjiang Plain based on an improved projection pursuit model. Natural Hazards 2016;82:683-701.

Prathumchai K, Honda K, Nualchawee K. Drought risk evaluation using remote sensing and GIS: A case study in Lop Buri Province. Proceedings of the 22nd Asian Conference on Remote Sensing; 2001 Nov 5-9; Singapore; 2001.

Saaty RW. The analytic hierarchy process-What it is and how it is used. Mathematical Modeling 1987;9(3-5):161-76.

Sehgal VK, Dhakar R. Geospatial approach for assessment of bioeconomic vulnerability to agricultural drought and its intraseasonal variations. Environmental Monitoring Assessment 2016;188(3):Article No. 197.

Senapati U, Das TK. Geospatial assessment of agricultural drought vulnerability using integrated three-dimensional model in the upper Dwarakeshwar River Basin in West Bengal, India.

Environmental Science and Pollution Research 2024; 31(41):54061-88.

Shahid S, Behrawan H. Drought risk assessment in the western part of Bangladesh. Natural Hazards 2008;46:391-413.

Smit B, Burton I, Klein RJ, Street R. The science of adaptation: A framework for assessment. Mitigation and Adaptive Strategies for Global Change 1999;4:199-213.

Sönmez FK, Komuscu AU, Erkan A, Turgu E. An analysis of spatial and temporal dimensions of drought vulnerability in Turkey using the standardized precipitation index. Natural Hazards 2005;35:243-64.

Tadesse T, Wardlow B, Svoboda M, Brown J. The vegetation outlook (VegOut): A new method for predicting vegetation seasonal greenness. GIScience and Remote Sensing 2010;47(1):25-52.

Tsangaratos P, Pizpikis T, Vasileiou E, Pliakas F, Schuth C, Kallioras A. Development of multi-criteria decision support system (DSS) coupled with GIS for identifying optimal locations for soil aquifer treatment (sat) facilities. Proceedings of the 13th International Congress; 2013 Sep; Chania, Greece; 2013.

United Nations Convention to Combat Desertification (UNCCD). Global Drought Snapshot 2023. The Need for Proactive Action, UNCCD; 2023; p. 38.

Vicente-Serrano SM, Begueria S, Lopez-Moreno JI. A Multi-scalar drought index sensitive to global warming: The standardized precipitation evapotranspiration index. Journal of Climate 2010;23:1696-718.

World Bank Group. Thailand Economic Monitor: Coping with Droughts and Floods; Building a Sustainable Future. Bangkok: World Bank; 2023.

World Meteorological Organization (WMO). Standardized Precipitation Index User Guide. Geneva: WMO-No. 1090; 2012. p. 24.